HHS Public Access

Author manuscript

J Bone Miner Res. Author manuscript; available in PMC 2022 December 01.

Published in final edited form as:

J Bone Miner Res. 2021 December ; 36(12): 2426–2439. doi:10.1002/jbmr.4447.

TNF-polarized macrophages produce insulin like 6 peptide to stimulate bone formation in rheumatoid arthritis in mice

Xiangjiao Yi[1,#], **Xin Liu**[1,#], **H. Mark Kenney**[1,#], **Rong Duan**[1], **Xi Lin**[1], **Edward Schwarz**[1,2], **Zhenqiang Yao**[1,*]

[1]Department of Pathology and Laboratory Medicine, and Center for Musculoskeletal Research, University of Rochester Medical Center, Rochester, NY 14642, USA;

[2]Department of Orthopedic Surgery, and Center for Musculoskeletal Research, University of Rochester Medical Center, Rochester, NY 14642, USA;

Abstract

The risk of osteoporosis is increased in rheumatoid arthritis (RA). Anti-TNF therapy has markedly improved the outcomes of RA patients, but does not improve osteoporosis in some reports. This could be a combined result of disease severity and other therapeutic agents, such as glucocorticoids that accelerate osteoporosis progression. We evaluated the effects of anti-TNF therapy on osteoporosis in an animal model of RA and explored the possible mechanisms involved. 6-week-old TNF transgenic (TNF-Tg) mice with early-stage erosive arthritis were treated with TNF antibody (Ab) or control IgG weekly for 4 weeks. We found that TNF Ab completely blocked the development of erosive arthritis in TNF-Tg mice, but only slightly increased vertebral bone mass, associated with reduction in parameters of both bone resorption and formation. Similarly, TNF Ab slightly increased trabecular bone mass in tibiae of 8-month-old TNF-Tg mice with advanced erosive arthritis. Interestingly, TNFα increased osteoblast differentiation from mouse bone marrow stromal cells (BMSCs) containing large number of macrophages, but not from pure mesenchymal progenitor cells (MPCs). TNFα-polarized macrophages (TPMs) did not express iNos and Arginase 1, typical markers of inflammatory and resident macrophages. Interestingly, TPMs stimulated osteoblast differentiation, unlike resident and inflammatory macrophages polarized by IL-4 and interferon-λ, respectively. RNA-seq analysis indicated that TPMs produced several anabolic factors, including Jagged1 and insulin like 6 (INSL6). Importantly, inhibition of either Jagged1 or INSL6 blocked TNFα-induced osteoblast differentiation. Furthermore, INSL6 Ab significantly decreased the expansion of TNF-induced MPCs in BMSCs, and anti-TNF Ab reduced INSL6 expression by macrophages in vitro and in TNF-Tg mice in vivo. We conclude that TPMs produce INSL6 to stimulate bone formation and

[*]Correspondence to: Zhenqiang Yao, PhD, Phone: (585) 275-8532; Fax: (585) 756-4468; zhenqiang_yao@urmc.rochester.edu, Department of Pathology and Laboratory Medicine, 601 Elmwood Ave, Box 626, Rochester, NY 14642, USA.

Author contributions: XY performed and analyzed the experiments in Figs 1&3. Xin Liu performed and analyzed the experiments in Figs 4&5. Mark Kenney performed and analyzed the experiments in Fig.2. RD helped in the analysis of the experiments in Figs 1&3 as well as Fig.6. Xi Lin analyzed the data in Fig.5A. ZY conceived and coordinated the studies, interpreted the results of all experiments and wrote the paper. All authors reviewed the results and approved the final version of the manuscript.

[#]These authors contribute equally to this work.

Competing interests: The authors declare there are no potential conflicts of interest.

anti-TNF Ab blocks not only enhanced bone resorption, but also the anabolic effect of TPMs on bone, limiting its effect to increase bone mass in this model of RA.

Keywords

osteoporosis; autoimmune arthritis; TNF-transgenic mice; anti-TNF therapy; bone turnover; osteoclast; osteoblast

Osteoporosis is one of the major aging diseases characterized by decreased bone mass and strength, leading to brittle, fragile bones and increased risk of fractures[1]. The risk of bone loss and fracture is increased in individuals with rheumatoid arthritis (RA) and other autoimmune diseases. Indeed, 2/3 of RA patients have osteoporosis and/or osteopenia compared with age-matched healthy control subjects with normal bone mass[2]. Osteoporosis is prone to occur in RA patients because osteoclasts, mediated by inflammatory factors, such as TNFα and IL-1β, induce not only erosion of cartilage and bone locally in affected joints, but also degradation of bone systemically[3]. These inflammatory factors promote the production of RANKL, an essential factor for terminal osteoclast differentiation and activation[4,5]. In addition, pain and loss of joint function in RA patients accelerates bone loss[3]. Furthermore, medications prescribed for RA patients, in particular, glucocorticoids, significantly accelerate bone loss[2] and decrease bone strength[6] by stimulating bone resorption and inhibiting bone formation[7].

In the past two decades, anti-TNF therapies have significantly improved outcomes for RA patients, but they have not provided a complete cure or lasting remission[8,9]. Some reports show that TNF inhibitors increase bone mineral density (BMD), associated with decreased markers of bone resorption and increased markers of bone formation[10,11]. But other reports show that TNF inhibitors do not increase new bone formation[12] and long-term treatment with TNF inhibitors even increase the rate of fracture, although BMD is increased in patients with ankylosing spondylitis who are treated with these agents[13]. Lee et al found that anti-TNF therapy did not increase lumbar and femoral neck BMD in RA patients also receiving a bisphosphonate (BP)[14]. Lumbar and femoral neck BMD was even reduced after short-term anti-TNF therapy in patients with RA[15]. Many factors, including disease severity or activity and glucocorticoid treatment, which accelerates bone loss, could influence the effect of anti-TNF agents on bone mass in RA patients[2,6,14,16] and explain the discrepancies in these reported outcomes. Here, we administered TNF antibody (Ab) to TNF transgenic (TNF-Tg) mice with erosive arthritis, which is accompanied by systemic bone loss[17,18], to evaluate the effects of it alone in a model of RA and explore the possible mechanisms involved.

Results

TNF Ab blocks the development of erosive arthritis, but has limited effect to increase trabecular bone mass in juvenile TNF-Tg mice with early arthritis.

At 6-weeks-old, the TNF-Tg mice did not have visible joint deformation. Two weeks later, mild toe and finger deformation was observed in some mice, but the deformation score was

not significantly different between IgG- and TNF Ab-treated mice (Fig.1A). After 3 and 4 weeks, the joint deformation score had sharply increased in the IgG control group, but remained low in the TNF Ab-treated mice ($p < 0.01$ vs. IgG, Fig.1A).

Histologic examination showed that the hind paws of 6-week-old TNF-Tg mice had mild inflammation and focal cartilage erosion in the carpal bones (Fig.1B) and some osteoclasts in the eroded bones (Fig.1C), indicating that 6-wk-old TNF-Tg mice have early erosive arthritis. After 4 wk of treatment, the wrist joint space in IgG-treated 10-wk-old TNF-Tg mice was heavily infiltrated with inflammatory cells, which invaded into the marrow cavity of the carpal bones, and the articular cartilage in some carpal bones was completely eroded (Fig.1B). In contrast, there was no cartilage or bone erosion in the wrist joints of mice treated with anti-TNF Ab (Fig.1B). Large numbers of osteoclasts were present on the eroded bone surfaces in the wrist joints of TNF-Tg mice treated with IgG, while few osteoclasts were present in the joints of TNF-Tg mice treated with anti-TNF Ab (Fig.1C).

Micro-CT analysis showed that vertebral trabecular bone mass (BV/TV) in 6-wk-old TNF-Tg was lower than that in WT littermates (Fig.1D). After 4 wk of treatment when the mice were 10-wk-old, vertebral BV/TV in WT mice was significantly higher than that in WT mice at baseline due to increased trabecular number and thickness (Fig.1D). Similarly, vertebral BV/TV in 10-wk-old TNF-Tg mice (IgG treated) was also significantly higher than in TNF-Tg mice at baseline (Fig.1D), indicating that vertebral bone mass increases during this rapid growth phase in both WT and TNF-Tg mice. The BV/TV value in TNF-Tg mice was 0.3-fold higher (22.07% vs 16.93%) in the mice given TNF Ab than in those given IgG treatment (Fig.1D), while it was 0.53-fold lower (16.93% vs 25.97%) compared to that of WT littermate mice. The BV/TV values in TNF-Tg mice, treated with either TNF Ab or IgG, were still significantly lower than those in WT littermates (Fig.1D).

Histomorphometric analysis indicated that the increase in trabecular bone volume in the proximal part of the tibiae of juvenile WT and TNF-Tg mice (Supplemental Fig.1) was similar to that in vertebrae. However, tibial trabecular BV/TV in 10-wk-old TNF-Tg mice treated with TNF Ab was not different from those TNF-Tg mice treated with IgG (Supplemental Fig.1) probably because histomorphometric analysis of bone volume is evaluated in the central part of the tibiae and does not include all of the trabecular bone, as evaluated by micro-CT.

TNF Ab has limited effect to increase trabecular bone mass in adult TNF-Tg mice with advanced erosive arthritis.

RA and other autoimmune diseases typically develop in older adults[19]. In TNF-Tg mice, erosive arthritis begins in juveniles (about 6 wks-old) and becomes severe in small joints, including in paws (Fig.1A) in young adults (2–3 month-old)[18] and in large joints, like knees, in 4–6m-old mice[20]. We also evaluated if TNF Ab could increase bone mass in osteoporotic adult TNF-Tg mice with severe erosive arthritis. 8-m-old TNF-Tg mice were used because their knee joints also have severe inversible erosion. We found that TNF Ab still significantly reduced the erosive area of the femoral surface of the patellofemoral joint (Fig.2B). As in the juvenile TNF-Tg mice, TNF Ab slightly increased trabecular bone volume in the tibial secondary spongiosae of 4 (8 legs) of the 5 adult TNF-Tg mice, but

BV/TV values in Ab-treated TNF-Tg mice was much lower than that in WT mice (Fig.2B). BV/TV in these TNF-Tg mice decreased 2.9-fold (7.04% vs 27.8%) compared to WT mice, while in the Ab-treated mice BV/TV increased only 0.68-fold (11.3% vs 7.04%). However, the 2 legs in the same one TNF-Tg mice (1 in the 5) treated with Ab had normal tibial BV/TV (Fig.2B). This was unusual. We were unable to know if this TNF-Tg mouse had never had lost bone or if the lost bone was restored.

TNF Ab decreases both bone resorption and formation in TNF-Tg mice.

Levels of the serum bone resorption marker, CTX1, and of the bone formation marker, P1NP, were significantly higher in 6-wk-old TNF-Tg mice than in their WT littermates (Fig.3A). After 4 wk of treatment, serum levels of both CTX1 and P1NP remained elevated in IgG-treated TNF-Tg (Fig.3A), but were significantly lower in TNF Ab-treated than in IgG-treated TNF-Tg mice (Fig.3A), suggesting that TNF Ab therapy reduced bone turnover.

Histomorphometric analysis showed that osteoclast numbers and surfaces were significantly higher in 6-week-old TNF-Tg mice than in their WT littermates (Fig.3B). Osteoclast surfaces were also significantly higher in IgG-treated TNF-Tg mice than in WT littermates (Fig.3B). Importantly, TNF Ab treatment significantly reduced osteoclast numbers and surfaces in TNF-Tg mice (Fig.3B).

Osteoblast surfaces in both 6- and 10- wk-old IgG-treated TNF-Tg mice trended towards an increase, but the differences did not reach statistical significance compared to their WT littermates (Fig.3C). However, osteoblast surfaces were significantly lower in TNF Ab-treated TNF-Tg mice than in IgG-treated TNF-Tg mice (Fig.3C). Bone formation rates (BFRs) were increased in 10-week-old IgG-treated TNF-Tg mice due to increased double-labeled surfaces and mineral apposition rates (MARs) compared to WT littermate mice (Fig.3D). TNF Ab significantly reduced the BFR due to reduced mineralizing surfaces and MARs compared to IgG treatment in TNF-Tg mice (Fig.3D).

TNFα-polarized macrophages (Macs) promote osteoblast differentiation.

We found that ~40% of so-called primary BMSCs cultured from C57Bl6 mice are $CD45^-$ mesenchymal progenitor cells (MPCs) and 56% of them are $CD45^+$ hemopoietic lineage cells, of which 75% (42% of the total cells) are $F4/80^+$ Macs (Fig.4A). About 10–15% of BMSCs were non-Macs hemopoietic cells (Fig.4A). Most of them were $Ly6C^+$ cells (Supplemental Fig.2A), of which about 1/3 were $Ly6G^+$ granulocytes (Supplemental Fig.2B), while there were few $B220^+$ B cells, $CD4^+$ T cells and $CD8^+$ T cells (Fig.2B&C). TNFα was added during expansion of BMSCs, which were then cultured in OB differentiation medium without TNFα. We found that BMSCs containing Macs pre-treated with 1–10 ng/ml of TNFα had enhanced ALP^+ OB differentiation (Fig.4B) and mineralized nodule formation (Supplemental Fig.3A) compared to BMSCs without TNFα pre-treatment. In contrast, pre-treatment of BMSCs with M-CSF did not change their potential for OB differentiation (Fig.4C) and mineralized nodule formation (Supplemental Fig.3B). Of note, 1–3 ng/ml of TNFα did not change OB differentiation from pre-treated pure MPCs, while 10ng/ml of TNFα reduced it (Fig.4D). Interestingly, TNFα kept the % of $F4/80^+$ Macs high and reduced the % of $Ly6G^+$ granulocytes in BMSCs (Supplemental Fig.2A&B).

During induction of OB differentiation from these BMSCs, the % of F4/80$^+$ Macs was further increased (Supplemental Fig.2A), while the % of Ly6G$^+$ granulocytes was reduced (Supplemental Fig.2B). Importantly, in the presence of TNFα-polarized Macs (T-Macs) but not M-CSF-induced Macs (M-Macs) from peripheral blood mononuclear cells (PBMCs), the pMPCs had significantly increased ALP$^+$ OB differentiation (Fig.4E). Of note, almost 100% of these M-Macs and T-Macs from PBMCs were CD45$^+$F4/80$^+$Ly6G$^-$ Macs (Supplemental Fig.4). These findings suggest that TNFα stimulates OB differentiation from BMSCs through polarized macrophages.

Macs are classified as inflammatory (M1) and resident (M2) cells, and are linked to Th1- and Th2-type immune responses, respectively[21]. The majority of Macs polarized by TNFα expressed the M1 marker, Ly6C^{++}, similar to our previous report[22], and almost 100% of F4/80$^+$Ly6C^{++} cells polarized by TNFα also expressed the recently identified M1 marker, CD38[23] (Fig.4F). As positive controls, IFN-γ-polarized M1s were also F4/80$^+$Ly6C^{++}CD38$^+$ cells (Fig.4F), while the majority of M-CSF-generated and IL-4-polarized M2s were Ly6C$^-$CD206$^+$ cells (not shown). However, unlike IFN-γ-polarized M1s, which typically express iNos, TNFα-polarized F4/80$^+$Ly6C^{++}CD38$^+$ Macs did not produce iNos (Fig.4F). In addition, 60% of TNFα-polarized F4/80$^+$Ly6C^{++}CD38$^+$ cells also expressed the M2 surface marker, CD206 (Fig.4F), but they did not have increased production of arginase 1 (Arg1, Fig.4G), which is different from typical IL-4-polarized Ly6C$^-$ M2s that produced large amount of Arg 1 (Fig.4G). Real-time PCR showed that compared to M-CSF treatment alone, addition of TNFα short-term (4 hr) increased the expression of the M1 marker genes, iNos, TNFα and IL-1β, ~10-fold in the macrophages, while expression of these genes decreased to levels similar to those cells treated with M-CSF alone at 24 hrs (Supplemental Fig.5). TNFα did not increase the expression of Stat1 at either 4 or 24 hr, and overall, it did not increase the expression of the M2 marker genes, Arg1, PPAR-γ and IL-10, at both time points (Supplemental Fig.5).

TNF-Tg mice have a higher % of CD11b$^+$Ly6G (Gr1)$^-$ myeloid cells in BM than WT mice, and 80% of these are F4/80$^+$ Macs (Supplemental Fig.6). We previously named CD11b$^+$Ly6G (Gr1)$^-$ myeloid cells OC precursors because they form many OCs in response to RANKL[24]. The % of CD38$^+$ (Ly6C$^-$) population was increased, but the % of Ly6C^{++}CD38$^{-/+}$ cells was reduced in CD11b$^+$Ly6G$^-$F4/80$^+$ Macs from TNF-Tg mice (Supplemental Fig.6). In general, the % of BM Macs, whether Ly6C high, low or negative, from both WT and TNF-Tg mice expressing IFN-γ was low, although Ly6C$^-$ Macs from both WT and TNF-Tg mice had a higher % expressing IFN-γ, and short-term treatment with TNF Ab did not reduce the % of IFN-γ$^+$ cells (Supplemental Fig.7).

Interestingly, however, different from TNFα-polarized Macs, which enhanced OB differentiation (Fig.4H), neither IL-4-polarized M2s nor IFN-γ-polarized M1s in the BMSCs stimulated OB differentiation and mineralized nodule formation (Fig.4H). In fact, IL-4-polarized M2s slightly inhibited ALP$^+$ OB differentiation (Fig.4H).

TNFα-polarized Macs produce insulin-like 6 peptide (INSL6) to stimulate OB differentiation by expanding mesenchymal progenitor cells (MPCs).

We cultured BM cells from C57Bl6 mice with M-CSF or M-CSF+TNFα to expand macrophages for RNA sequence analysis in order to identify factors produced by TNFα-polarized macrophages that stimulate OB differentiation. Among the signaling pathways, BMP, Wnt, FGF, Notch and IGF that are known to regulate OB differentiation, we found that the expression of Wnt9a, INSL6, Wnt6 and Jagged 1 were >2-fold increase in TNFα-polarized macrophages compared to those induced by M-CSF (Fig.5A). However, the basal level of Wnt9a was very low and we did not test it further. In contrast, the expression levels of BMP2, FGF1, FGF2 and Jagged 2 were actually reduced in TNFα-polarized Macs (Fig.5A). Real-time PCR confirmed that the expressions of INSL6 and Jagged 1 were increased (Fig.5B), while the expression of Wnt6 was undetectable (not shown) in TNFα-polarized macrophages. Importantly, addition of either Jagged 1 or INSL6 Ab completely prevented the increase in OB differentiation in mouse BMSCs induced by TNFα-polarized Macs and also reduced ALP^+ OB area compared to control BMSCs (Fig.5C), suggesting that Jagged 1 and INSL6 produced by TNFα-polarized macrophages play a critical role in the anabolic effects of TNFα in bone.

We are unaware of any reports showing a role for INSL6 in bone cells, while Jagged 1 is known to be essential for osteoblast differentiation and maintenance of the osteoblastic osteoprogenitor pool[25,26]. We expanded BMSCs in 6-well plates, which were pre-coated with IgG or INSL6 Ab, to determine if INSL6 produced by TNFα-polarized macrophages promotes the expansion of MPCs by analyzing $CD45^-F4/80^-$ MPCs. Addition of TNFα significantly increased the total number of MPCs, although it reduced the % of MPCs from −47% to −35% (Fig.5D) because it significantly increased the total number of cells (not shown). The % of MPCs in the wells coated with INSL6 Ab was sharply reduced to −10% in both control and TNFα-treated BMPCs, and the total numbers of MPCs were also significantly reduced in INSL6 Ab-coated wells (Fig.5D).

Anti-TNF therapy reduces INSL6 expression by macrophages.

To determine if anti-TNF therapy inhibits the expression of INSL6 by macrophages, we first cultured WT mouse BMSCs with TNFα or M-CSF in the presence of TNFα Ab or TNF receptor IgG Fc[27,28] to test their expression of INSL6 mRNA. INSL6 mRNA expression was significantly increased in TNFα-treated BMSCs containing Macs compared to those without TNFα treatment and to M-CSF-induced Macs (Fig.6A). Addition of either TNFα Ab or TNFα receptor IgG Fc almost completely blocked TNFα-induced INSL6 expression (Fig.6A). Nest, we tested if anti-TNF therapy reduced INSL6 expression in TNF-Tg mice in vivo. INSL6-expressing Macs were present in small numbers in the BM of the WT mice and were markedly increased in the BM of TNF-Tg mice (Fig.6). INSL6 was also expressed on non-Mac cells in the BM of both WT and TNF-Tg mice. Of note, few $INSL6^+$ cells were distributed on trabecular surfaces, which is consistent with our finding that the major role of INLS6 is to expand MPCs (Fig.5D). Importantly, $INSL6^+$ Macs and non-Mac cells were markedly reduced in the BM of TNF Ab-treated mice (Fig.6B).

Discussion

Our findings establish a novel paradigm for the coupling of bone formation to resorption through TNFα-polarized Macs, which not only have enhanced potential to destroy bone by forming osteoclasts in response to RANKL[22], but also to exert anabolic effects in bone by producing osteoblast-stimulating factors during bone remodeling in our TNF-Tg mouse model of rheumatoid arthritis. This paradigm could potentially also be applicable to postmenopausal and age-related osteoporosis, in which TNFα levels also are increased[29–31]. The anabolic effect of TNFα-polarized Macs could be an important mechanism to slow down bone loss in rheumatoid diseases. Based on this paradigm, it is not difficult to understand a previous clinical observation that osteoporosis is not improved in RA patients by anti-TNF therapy[10,12,14,15] because it not only blocks the enhanced bone resorption on trabeculae, but also the basic anabolic effect of TNFα on bone. In 6-week-old TNF-Tg mice with early-stage erosive arthritis, 4 weeks of TNF Ab treatment completely blocked the joint inflammation and erosion, but it only partially increased trabecular bone volume, associated with reduced parameters of both bone resorption and formation. The slightly increased trabecular bone volume in juvenile TNF-Tg mice after TNF Ab treatment likely resulted from growth-associated new bone formation during this rapid phase of bone modeling when TNF Ab blocked local and systemic inflammation and associated enhanced bone resorption. In adult TNF-Tg mice with inversible erosive arthritis, the effects of TNF Ab to increase trabecular bone volume were also limited. The tibial bone volume was increased only 0.68-fold in the TNF-Tg mice after TNF Ab treatment (11.8% vs 7.04%). In contrast, it decreased 2.9-fold (7.04% vs 27.6%) in the adult TNF-Tg mice treated with vehicle compared to WT littermate mice. Thus, our findings suggest that an anabolic agent could be given together with anti-TNF therapy to increase bone in patients with RA.

Bone formation and resorption are coupled, not only in physiologic, but also in pathologic conditions. For example, in postmenopausal osteoporosis, both resorption and formation are increased[32–34], but resorption exceeds formation, resulting in bone loss[35]. In juvenile TNF-Tg mice, inflamed joints are actively eroded (Fig.1), associated with increased systemic bone resorption parameters (Fig.3A&B). Bone formation parameters, including serum PINP, osteoblast surface and dynamic bone formation rates, are also increased in these juvenile TNF-Tg mice (Fig.3C, D&E), while bone formation is reduced in old TNF-Tg mice[36]. TNFα induces osteoclastogenesis, not only indirectly by stimulating RANKL production by accessory cells[37], but also directly by sequentially activating NF-κB, c-Fos followed by NFATc1, similar to and independent of RANKL[18,38]; it can also regulate bone formation both negatively and positively by activating NF-κB RelA[39,40]. Indeed, at appropriate doses, TNFα promotes fracture repair by augmenting the recruitment and differentiation of stromal cells[41]. Here, we have provided the first evidence that TNF-polarized macrophages can directly promote coupling of bone formation to the enhanced bone resorption by producing bone anabolic factors, including INSL6 and jagged 1 (Fig.5). Jagged 1 is one of the five ligands for receptors in Notch signaling, which is an important determinant of cell fate and is active throughout development and across many organ systems[42]. In general, Notch activation results in enhanced polarization of T helper cells 1 and 17, osteoclast differentiation and macrophage activation, which all promote the progression of rheumatoid

diseases, although inhibitory effects of Jagged 1 on the progression of rheumatoid arthritis have also been reported[43]. We have made the novel observation that TNF-polarized macrophages produce Jagged 1 to slow down systemic bone loss by stimulating bone formation in our animal model of rheumatoid arthritis. This is consistent with the known biological function of Jagged 1 to stimulate osteoblast differentiation and maintain the osteoblastic osteoprogenitor pool[25,26]. INSL6, a member of the insulin family of proteins, is highly expressed in the testis[44] and is critical for spermatogenesis[45]. INSL6 also prevents cardiac fibrosis, and thus continuous INSL6 infusion attenuates left ventricular systolic dysfunction induced by isoproterenol[46]. Ours is the first report showing an anabolic effect of INSL6 in bone. INSL6 produced by TNFα-polarized macrophages stimulates bone formation by expanding mesenchymal progenitor cells and increasing osteoblast formation (Fig.5A–D). TNF Ab markedly reduced the expression of INSL6 by both Macs and non-Mac cells in BM (Fig.6B) and thus limited INSL6's anabolic effect in bone. Further studies will be required to fully characterize these non-Mac cells.

Inflammatory Macs induce inflammation, while resident Macs are involved in tissue repair. Our findings suggest that TNFα-polarized Macs are also important for tissue repair. Macs have been implicated in ectopic bone formation, such as osteophyte formation in osteoarthritis and arteriole calcification by producing BMP2, BMP4, TGFβ1[47,48]. A type of tissue resident (M2) Macs, called OsteoMacs, are associated with and maintain osteoblasts at bone remodeling sites[49] and stimulate fracture repair[50]. M-CSF is a critical factor for generation of Macs, which have a M2 phenotype and are further polarized by IL-4[51,52]. Our findings indicate that M-CSF-generated Macs do not stimulate or inhibit OB differentiation (Fig. 4C), nor does IL-4-polarized M2s in BMSCs (Fig.4H). This is consistent with a previous report that IL-4 inhibits OB differentiation[53]. Interestingly, typical M1s polarized by IFN-γ do not stimulate OB differentiation (Fig.4H). Compared to M-CSF generated Macs, TNFα-polarized Macs have increased expression of a number of anabolic factors, including Jagged 1 and Insl6 (Fig.5A–C), which are critical for their anabolic effect (Fig.5D).

Our in vitro and in vivo findings suggest that TNFα-polarized Macs cannot be simply classified as traditional M1s or M2s. We have not found a specific marker to distinguish TNFα-polarized Macs from those polarized by IFN-γ and LPS (not shown). Although the majority of TNFα-polarized F4/80$^+$ Macs express the M1 markers, Ly6C[54] and CD38[55], in vitro similar to those polarized by IFN-γ (Fig.4F), BM CD11b$^+$Ly6G$^-$F4/80$^+$ Macs from TNF-Tg mice have an increased % of CD38$^+$Ly6C$^-$ cells, but not of Ly6C^{++}CD38$^+$ cells compared to those from WT littermate mice (Supplemental Fig.6) probably because M-CSF, which induces Ly6C$^-$ Macs (Fig.4F), is predominant in BM of TNF-Tg mice, although the level of TNFα is also increased[24]. In addition, some TNFα-polarized Ly6C^{++}CD38$^+$ Macs also express the M2 marker, CD206 (Fig.4F). Furthermore, few TNFα-polarized Ly6C^{++}CD38$^+$ Macs produce the traditional M1 marker, iNOS (Fig.4F), which inhibits bone formation[56,57]; this is consistent with the in vivo findings that few BM Macs from either WT or TNF-Tg mice express iNos, and TNF Ab does not reduce the expression of iNos in BM Macs from TNF-Tg mice (Supplemental Fig.7).

TNFα-mediated anabolic effects on bone are important because they could partly compensate for the increased bone resorption and slow down bone loss in diseases, such as postmenopausal osteoporosis[32–34]. Blocking the anabolic effects of TNF-polarized Macs by anti-TNF agents could be challenging for the management of osteoporosis in RA patients. Similar to anti-resorptive agents, bisphosphonate and denosumab[58–60], anti-TNF therapy also inhibits both bone resorption and formation. Thus, combining an anti-TNF agent and a bisphosphonate does not have additional benefits to increase bone mass compared to bisphosphonate alone in RA patients[14]. Similarly, anti-TNF agents have very limited effects to increase BMD in RA patients when they are combined with denosumab[61]. The anabolic agent, teriparatide, is recommended as a second line agent if first line therapy fails in the treatment of osteoporosis in rheumatoid diseases[62]. However, PTH levels are significantly increased in RA patients, associated with radiographic evidence of typical bony erosions[63], and teriparatide does not improve joint erosion in RA patients[64]. Thus, the rationale for using Teriparatide to treat osteoporosis in RA patients should be re-evaluated. Our findings suggest that a novel anabolic agent is required to counteract the inhibitory effects of anti-TNF therapy on the anabolic effects of TNF-polarized macrophages in RA patients with osteoporosis.

Material and Methods

Animals and drug administration:

TNF-transgenic (TNF-Tg) mice (line 3647 generated by the Kollias group[17]), which develop progressive erosive arthritis, accompanied by increasing bone loss, were used in this study. All experimental protocols, the use and care of animals were approved by the University of Rochester Committee for Animal Resources and all methods were carried out in accordance with the guidelines and regulations of the American Veterinary Medical Association (AVMA). The mice were housed in micro-isolator cages under specific pathogen-free conditions.

Female TNF-Tg mice develop RA earlier with a more severe and consistent arthritic phenotype than male mice. Thus, 6-week-old female TNF-Tg mice on C57Bl6 background with early stage RA, as we reported[18], were randomly divided into 2 treatment groups: 1) normal IgG control; and 2) TNF Ab, 8 mice/group, and were intraperitoneally injected once a week with 10 mg/kg of normal IgG 2a/kappa or anti-TNF monoclonal antibody (Janssen, Spring House, PA, USA)[65], respectively, for 4 weeks. Control WT littermate mice were un-treated. The progression of arthritis was blindly evaluated weekly by the joint deformation score we developed previously[18]. Mice were I.P. injected with 5 mg/kg of Calcein (Sigma, C-0875) and Alizarin Complexone dihydrate (ACROS, cat# 155830010) at 5 d and 1 day, respectively, before sacrifice, following our standard protocol[18,66]. In addition, 6-week-old female TNF-Tg and their WT littermates were euthanized at baseline. To evaluate the effect of anti-TNF therapy on the osteoporotic bone in adult RA, 8-m-old male TNF-Tg mice with severe inversible joint erosion were randomly divided into two groups, which were given normal IgG or TNF Ab, respectively, and the WT littermate mice were given PBS, for 6 weeks as above.

Histomorphometric analysis:

Paraffin-processed hind-paw sections with good exposure of carpal bones were selected from a series of representative sections for H&E and TRAP staining for histologic evaluation of inflammation and joint erosion, and osteoclast formation, respectively. Representative sections cut through the center of the proximal shaft of the tibiae were selected from a series of sections for histomorphometric analysis of bone structural parameters and osteoblasts, and of osteoclasts on H&E- and TRAP-stained sections, respectively. Right legs were processed undecalcified and embedded in plastic to evaluate dynamic parameters of bone formation[18,66]. Tissue staining and slide selection and all histomorphometric parameters were evaluated blindly by an independent investigator who was not involved in the experiment, using OsteoMeasure software[18,66] following the guidelines of the ASBMR Histomorphometry Nomenclature Committee[67].

Micro-CT evaluation:

The spines and knee joints were scanned using a Viva CT 40 instrument (Scanco Medical) to determine trabecular bone structural parameters in L1 vertebrae and in a 200 μm-long region starting at 100 μm beneath the growth plate, according to JBMR standard guidelines[68].

Erosion of the anterior surface of the distal femur centered on the patellofemoral joint was evaluated using Amira software (v.2020.2; ThermoFisher Scientific, Hillsboro, OR, USA). Briefly, the patella segmented by the magic wand tool was removed from the dataset by setting the threshold mask of the voxels with a lower limit of 2500 Hounsfield units (HU). If the patella-associated voxels remained connected to those of the femur with a mask of 2500 HU, a lower limit >2500 HU was selected to isolate voxels specific to the interior portion of the patella as watershed seeds. To orient the anterior surface of the femur parallel to the x or y plane, the dataset was rotated using the Transform Editor. A Resample Transformed Image module was applied to the rotated dataset to create a new dataset oriented parallel to the x or y plane. The lasso tool was used to generate a polygon surrounding the erosive area on the anterior aspect of the femur and the selection was added to a new label field. A Material Statistics module was applied to the label field to extract the volume (mm^3) of the region of interest in the single slice, which was converted to area (mm^2) by the isotropic voxel size (0.0174 mm) representing the single slice length. Each limb was analyzed as a single data point and data are presented as mean ± standard deviation.

ELISA:

Levels of carboxy-terminal crosslinked telopeptide of type 1 collagen (CTX-1) and procollagen type 1 N-terminal pro-peptide (P1NP), specific biomarkers of bone resorption and formation, respectively[69], in serum samples, and arginase 1 in cell culture medium, were tested by ELISA, according to the manufacturer's instructions (MyBiosource, San Diego, CA).

In vitro osteoblast differentiation assay: 1×10^6 BM cells from C57Bl6 mice were seeded in each well of 12-well-plates with α-MEM containing 15% FBS, plus different doses of cytokines, for 5 d to expand bone marrow stromal cells (BMSCs) followed by induction of osteoblast differentiation with 25 μg/ml ascorbic acid (Vit-C) and 5 mM

β-glycerophosphate (β-GP)[66]. After 6 d, the cells were fixed in 10% neutral buffered formalin followed by ALP staining to measure ALP^+ cell area. Alternatively, the cells were counter-stained with eosin to measure the total cell area[70]. Similarly, pure mesenchymal progenitor cells (pMPCs), generated from mouse cortical bone[66], were used to test osteoblast differentiation by measuring ALP^+ cell area. For assessment of mineralized nodule formation, cultured cells were treated with OB differentiation for 12 d when nodules typically were visible and the cells were fixed with 10% neutral buffered formalin, followed by Von Kossa staining to measure the area of mineralized nodules.

RNA-sequence:

BM cells from C57Bl6 mice were cultured with 3 ng/ml of M-CSF alone or together with 3 ng/ml of TNFα for 3 d. Total RNA was extracted by Trizol reagent and RNA sequencing was performed on an Illumina HiSeq2500 high-throughput DNA sequencer (Illumina) in the Genomic Core at the University of Rochester. A threshold of differentially-expressed genes (DEGs) between the two groups was set as fold-change >2 and an adjusted p-value <0.05. Heatmap of genes for secreted proteins involved in osteoblast differentiation, including BMP, Wnt, FGF, Notch and IGF signaling pathways, was generated using rlog-transformed normalized counts after standardization across samples in the two groups.

Quantitative Real Time PCR: 1 μg of total RNA extracted from cultured cells by Trizol reagent was reversely transcribed to cDNA in a 20 μl reaction using an iSCRIPT cDNA Synthesis kit (Bio-Rad). The expression levels of *jagged1, INSL6* and actin were measured using an iCycler real-time PCR machine (Bio-Rad) with iQ SYBR SuperMix (Bio-Rad), according to the manufacturer's instructions.

Flow cytometry: Cultured bone marrow cells from C57Bl6 mice were digested using 0.25% trypsin to collect attached cells. To test cell surface markers, 1×10^6 cells from each sample were stained with fluorescence-conjugated Abs in FACS buffer (2% FBS in PBS) at 4°C for 30 min. To test intracellular markers, cells stained with surface markers were then fixed and permeabilized using BD Cytofix/Cytoperm solution kit (BD; Cat #: 51-2090/2091KZ), followed by incubation with fluorescence-conjugated Ab in 100 μl Perm/Wash buffer. The cells in FACS buffer were then immediately subjected to analysis using a flow cytometer (FACS LSR II; BD Biosciences). FlowJo software was used for data analysis.

Immunofluorescence.

Paraffin-embedded sections (4 μm thick) of decalcified leg bones were incubated with anti-mouse F4/80 monoclonal Ab (Biolegend #123102) and INSL6 Ab (Invitrogen #PA5106458) overnight at 4°C followed by Alexa Fluor 568- and Alexa Fluor 488-conjugated HRP-labeled secondary Ab (Abcam, #ab175475 and #ab150073) for 2 h at room temperature and DAPI (Vector #H-1200) counterstaining. The images were observed using a Zeiss fluorescence microscope.

Statistics: All data were performed normality test. Data were given as the mean ± S.D. when they were distributed normally. Median and interquartile range were used instead

when data distributions were skewed. Comparisons between two groups were analyzed using Student's two-tailed unpaired *t*-test and those among 3 or more groups using one-way analysis of variance followed by Dunnett's post-hoc multiple comparisons when data were distributed normally. In contrast, log transformed data were used to do statistical analysis when data distributions were skewed. p values <0.05 were considered statistically significant. Each in vitro experiment was repeated 3 times with similar results.

Supplementary Material

Refer to Web version on PubMed Central for supplementary material.

Acknowledgments:

Dr. Brendan Boyce provided consultant advice and language editing for this paper. The authors thank Lindsay Schnur for micro-CT imaging and analysis.

Funding:

The research was supported by National Institutes of Health (NIH) R01AG049994, and P30 AR069655. The content is solely the responsibility of the authors and does not necessarily represent the official views of the funding source.

Data availability statement.

The data that support the findings of this study are available from the corresponding author upon reasonable request.

References

1. Looker AC, Melton LJ, 3rd, Harris TB, Borrud LG, Shepherd JA. Prevalence and trends in low femur bone density among older US adults: NHANES 2005–2006 compared with NHANES III. Journal of bone and mineral research : the official journal of the American Society for Bone and Mineral Research 2010;25:64–71.
2. Hafez EA, Mansour HE, Hamza SH, Moftah SG, Younes TB, Ismail MA. Bone mineral density changes in patients with recent-onset rheumatoid arthritis. Clinical medicine insights Arthritis and musculoskeletal disorders 2011;4:87–94. [PubMed: 22084606]
3. Goldring SR, Gravallese EM. Mechanisms of bone loss in inflammatory arthritis: diagnosis and therapeutic implications. Arthritis Res 2000;2:33–7. [PubMed: 11094416]
4. Lacey DL, Timms E, Tan HL, et al. Osteoprotegerin ligand is a cytokine that regulates osteoclast differentiation and activation. Cell 1998;93:165–76. [PubMed: 9568710]
5. Dougall WC, Glaccum M, Charrier K, et al. RANK is essential for osteoclast and lymph node development. Genes & development 1999;13:2412–24. [PubMed: 10500098]
6. Takahata M, Maher JR, Juneja SC, et al. Mechanisms of bone fragility in a mouse model of glucocorticoid-treated rheumatoid arthritis: implications for insufficiency fracture risk. Arthritis and rheumatism 2012;64:3649–59. [PubMed: 22832945]
7. Canalis E Mechanisms of glucocorticoid-induced osteoporosis. Current opinion in rheumatology 2003;15:454–7. [PubMed: 12819474]
8. Taylor PC, Feldmann M. Anti-TNF biologic agents: still the therapy of choice for rheumatoid arthritis. Nature reviews Rheumatology 2009;5:578–82. [PubMed: 19798034]
9. Monaco C, Nanchahal J, Taylor P, Feldmann M. Anti-TNF therapy: past, present and future. Int Immunol 2015;27:55–62. [PubMed: 25411043]
10. Kawai VK, Stein CM, Perrien DS, Griffin MR. Effects of anti-tumor necrosis factor alpha agents on bone. Current opinion in rheumatology 2012;24:576–85. [PubMed: 22810364]

11. McMahon MS, Ueki Y. Does anti-TNF-alpha have a role in the treatment of osteoporosis? Bull NYU Hosp Jt Dis 2008;66:280–1. [PubMed: 19093904]
12. Baraliakos X, Haibel H, Listing J, Sieper J, Braun J. Continuous long-term anti-TNF therapy does not lead to an increase in the rate of new bone formation over 8 years in patients with ankylosing spondylitis. Annals of the rheumatic diseases 2014;73:710–5. [PubMed: 23505240]
13. Beek KJ, Rusman T, van der Weijden MAC, et al. Long-Term Treatment With TNF-Alpha Inhibitors Improves Bone Mineral Density But Not Vertebral Fracture Progression in Ankylosing Spondylitis. Journal of bone and mineral research : the official journal of the American Society for Bone and Mineral Research 2019;34:1041–8.
14. Lee JS, Lim DH, Oh JS, et al. Effect of TNF inhibitors on bone mineral density in rheumatoid arthritis patients receiving bisphosphonate: a retrospective cohort study. Rheumatol Int 2019.
15. Orsolini G, Adami G, Adami S, et al. Short-Term Effects of TNF Inhibitors on Bone Turnover Markers and Bone Mineral Density in Rheumatoid Arthritis. Calcified tissue international 2016;98:580–5. [PubMed: 26887973]
16. Lodder MC, de Jong Z, Kostense PJ, et al. Bone mineral density in patients with rheumatoid arthritis: relation between disease severity and low bone mineral density. Annals of the rheumatic diseases 2004;63:1576–80. [PubMed: 15547081]
17. Keffer J, Probert L, Cazlaris H, et al. Transgenic mice expressing human tumour necrosis factor: a predictive genetic model of arthritis. The EMBO journal 1991;10:4025–31. [PubMed: 1721867]
18. Yao Z, Xing L, Boyce BF. NF-kappaB p100 limits TNF-induced bone resorption in mice by a TRAF3-dependent mechanism. The Journal of clinical investigation 2009;119:3024–34. [PubMed: 19770515]
19. Helmick CG, Felson DT, Lawrence RC, et al. Estimates of the prevalence of arthritis and other rheumatic conditions in the United States. Part I. Arthritis and rheumatism 2008;58:15–25. [PubMed: 18163481]
20. Bell RD, Slattery PN, Wu EK, Xing L, Ritchlin CT, Schwarz EM. iNOS dependent and independent phases of lymph node expansion in mice with TNF-induced inflammatory-erosive arthritis. Arthritis research & therapy 2019;21:240. [PubMed: 31727153]
21. Mosser DM, Edwards JP. Exploring the full spectrum of macrophage activation. Nature reviews Immunology 2008;8:958–69.
22. Zhao Z, Hou X, Yin X, et al. TNF Induction of NF-kappaB RelB Enhances RANKL-Induced Osteoclastogenesis by Promoting Inflammatory Macrophage Differentiation but also Limits It through Suppression of NFATc1 Expression. PloS one 2015;10:e0135728. [PubMed: 26287732]
23. Jablonski KA, Amici SA, Webb LM, et al. Novel Markers to Delineate Murine M1 and M2 Macrophages. PloS one 2015;10:e0145342. [PubMed: 26699615]
24. Yao Z, Li P, Zhang Q, et al. Tumor necrosis factor-alpha increases circulating osteoclast precursor numbers by promoting their proliferation and differentiation in the bone marrow through up-regulation of c-Fms expression. The Journal of biological chemistry 2006;281:11846–55. [PubMed: 16461346]
25. Hill CR, Yuasa M, Schoenecker J, Goudy SL. Jagged1 is essential for osteoblast development during maxillary ossification. Bone 2014;62:10–21. [PubMed: 24491691]
26. Lawal RA, Zhou X, Batey K, et al. The Notch Ligand Jagged1 Regulates the Osteoblastic Lineage by Maintaining the Osteoprogenitor Pool. Journal of bone and mineral research : the official journal of the American Society for Bone and Mineral Research 2017;32:1320–31.
27. Lei W, Duan R, Li J, et al. The IAP Antagonist SM-164 Eliminates Triple-Negative Breast Cancer Metastasis to Bone and Lung in Mice. Sci Rep 2020;10:7004. [PubMed: 32332865]
28. Yao Z, Lei W, Duan R, Li Y, Luo L, Boyce BF. RANKL cytokine enhances TNF-induced osteoclastogenesis independently of TNF receptor associated factor (TRAF) 6 by degrading TRAF3 in osteoclast precursors. The Journal of biological chemistry 2017;292:10169–79. [PubMed: 28438834]
29. Zha L, He L, Liang Y, et al. TNF-alpha contributes to postmenopausal osteoporosis by synergistically promoting RANKL-induced osteoclast formation. Biomed Pharmacother 2018;102:369–74. [PubMed: 29571022]

30. Roggia C, Gao Y, Cenci S, et al. Up-regulation of TNF-producing T cells in the bone marrow: a key mechanism by which estrogen deficiency induces bone loss in vivo. Proceedings of the National Academy of Sciences of the United States of America 2001;98:13960–5. [PubMed: 11717453]
31. Ginaldi L, Di Benedetto MC, De Martinis M. Osteoporosis, inflammation and ageing. Immunity & ageing : I & A 2005;2:14. [PubMed: 16271143]
32. Garnero P, Shih WJ, Gineyts E, Karpf DB, Delmas PD. Comparison of new biochemical markers of bone turnover in late postmenopausal osteoporotic women in response to alendronate treatment. The Journal of clinical endocrinology and metabolism 1994;79:1693–700. [PubMed: 7989477]
33. Garnero P, Sornay-Rendu E, Chapuy MC, Delmas PD. Increased bone turnover in late postmenopausal women is a major determinant of osteoporosis. Journal of bone and mineral research : the official journal of the American Society for Bone and Mineral Research 1996;11:337–49.
34. Eriksen EF, Hodgson SF, Eastell R, Cedel SL, O'Fallon WM, Riggs BL. Cancellous bone remodeling in type I (postmenopausal) osteoporosis: quantitative assessment of rates of formation, resorption, and bone loss at tissue and cellular levels. Journal of bone and mineral research : the official journal of the American Society for Bone and Mineral Research 1990;5:311–9.
35. Marie PJ, Kassem M. Osteoblasts in osteoporosis: past, emerging, and future anabolic targets. European journal of endocrinology / European Federation of Endocrine Societies 2011;165:1–10.
36. Kaneki H, Guo R, Chen D, et al. Tumor necrosis factor promotes Runx2 degradation through up-regulation of Smurf1 and Smurf2 in osteoblasts. The Journal of biological chemistry 2006;281:4326–33. [PubMed: 16373342]
37. Lam J, Takeshita S, Barker JE, Kanagawa O, Ross FP, Teitelbaum SL. TNF-alpha induces osteoclastogenesis by direct stimulation of macrophages exposed to permissive levels of RANK ligand. The Journal of clinical investigation 2000;106:1481–8. [PubMed: 11120755]
38. Yamashita T, Yao Z, Li F, et al. NF-kappaB p50 and p52 regulate receptor activator of NF-kappaB ligand (RANKL) and tumor necrosis factor-induced osteoclast precursor differentiation by activating c-Fos and NFATc1. The Journal of biological chemistry 2007;282:18245–53. [PubMed: 17485464]
39. Hess K, Ushmorov A, Fiedler J, Brenner RE, Wirth T. TNFalpha promotes osteogenic differentiation of human mesenchymal stem cells by triggering the NF-kappaB signaling pathway. Bone 2009;45:367–76. [PubMed: 19414075]
40. Li Y, Li A, Strait K, Zhang H, Nanes MS, Weitzmann MN. Endogenous TNFalpha lowers maximum peak bone mass and inhibits osteoblastic Smad activation through NF-kappaB. Journal of bone and mineral research : the official journal of the American Society for Bone and Mineral Research 2007;22:646–55.
41. Glass GE, Chan JK, Freidin A, Feldmann M, Horwood NJ, Nanchahal J. TNF-alpha promotes fracture repair by augmenting the recruitment and differentiation of muscle-derived stromal cells. Proceedings of the National Academy of Sciences of the United States of America 2011;108:1585–90. [PubMed: 21209334]
42. Grochowski CM, Loomes KM, Spinner NB. Jagged1 (JAG1): Structure, expression, and disease associations. Gene 2016;576:381–4. [PubMed: 26548814]
43. Sucur A, Filipovic M, Flegar D, et al. Notch receptors and ligands in inflammatory arthritis - a systematic review. Immunol Lett 2020;223:106–14. [PubMed: 32325090]
44. Lok S, Johnston DS, Conklin D, et al. Identification of INSL6, a new member of the insulin family that is expressed in the testis of the human and rat. Biol Reprod 2000;62:1593–9. [PubMed: 10819760]
45. Burnicka-Turek O, Shirneshan K, Paprotta I, et al. Inactivation of insulin-like factor 6 disrupts the progression of spermatogenesis at late meiotic prophase. Endocrinology 2009;150:4348–57. [PubMed: 19520787]
46. Maruyama S, Wu CL, Yoshida S, et al. Relaxin Family Member Insulin-Like Peptide 6 Ameliorates Cardiac Fibrosis and Prevents Cardiac Remodeling in Murine Heart Failure Models. J Am Heart Assoc 2018;7.

47. Blom AB, van Lent PL, Holthuysen AE, et al. Synovial lining macrophages mediate osteophyte formation during experimental osteoarthritis. Osteoarthritis Cartilage 2004;12:627–35. [PubMed: 15262242]
48. Champagne CM, Takebe J, Offenbacher S, Cooper LF. Macrophage cell lines produce osteoinductive signals that include bone morphogenetic protein-2. Bone 2002;30:26–31. [PubMed: 11792561]
49. Chang MK, Raggatt LJ, Alexander KA, et al. Osteal tissue macrophages are intercalated throughout human and mouse bone lining tissues and regulate osteoblast function in vitro and in vivo. Journal of immunology 2008;181:1232–44.
50. Alexander KA, Chang MK, Maylin ER, et al. Osteal macrophages promote in vivo intramembranous bone healing in a mouse tibial injury model. Journal of bone and mineral research : the official journal of the American Society for Bone and Mineral Research 2011;26:1517–32.
51. Murai M, Turovskaya O, Kim G, et al. Interleukin 10 acts on regulatory T cells to maintain expression of the transcription factor Foxp3 and suppressive function in mice with colitis. Nature immunology 2009;10:1178–84. [PubMed: 19783988]
52. Mia S, Warnecke A, Zhang XM, Malmstrom V, Harris RA. An optimized protocol for human M2 macrophages using M-CSF and IL-4/IL-10/TGF-beta yields a dominant immunosuppressive phenotype. Scand J Immunol 2014;79:305–14. [PubMed: 24521472]
53. Riancho JA, Gonzalez-Marcias J, Amado JA, Olmos JM, Fernandez-Luna JL. Interleukin-4 as a bone regulatory factor: effects on murine osteoblast-like cells. Journal of endocrinological investigation 1995;18:174–9. [PubMed: 7542294]
54. Rahman K, Vengrenyuk Y, Ramsey SA, et al. Inflammatory Ly6Chi monocytes and their conversion to M2 macrophages drive atherosclerosis regression. The Journal of clinical investigation 2017;127:2904–15. [PubMed: 28650342]
55. Amici SA, Young NA, Narvaez-Miranda J, et al. CD38 Is Robustly Induced in Human Macrophages and Monocytes in Inflammatory Conditions. Frontiers in immunology 2018;9:1593. [PubMed: 30042766]
56. Cuzzocrea S, Mazzon E, Dugo L, et al. Inducible nitric oxide synthase mediates bone loss in ovariectomized mice. Endocrinology 2003;144:1098–107. [PubMed: 12586786]
57. Armour KJ, Armour KE, van't Hof RJ, et al. Activation of the inducible nitric oxide synthase pathway contributes to inflammation-induced osteoporosis by suppressing bone formation and causing osteoblast apoptosis. Arthritis and rheumatism 2001;44:2790–6. [PubMed: 11762939]
58. Delmas PD, Vergnaud P, Arlot ME, Pastoureau P, Meunier PJ, Nilssen MH. The anabolic effect of human PTH (1–34) on bone formation is blunted when bone resorption is inhibited by the bisphosphonate tiludronate--is activated resorption a prerequisite for the in vivo effect of PTH on formation in a remodeling system? Bone 1995;16:603–10. [PubMed: 7669436]
59. Mashiba T, Hirano T, Turner CH, Forwood MR, Johnston CC, Burr DB. Suppressed bone turnover by bisphosphonates increases microdamage accumulation and reduces some biomechanical properties in dog rib. Journal of bone and mineral research : the official journal of the American Society for Bone and Mineral Research 2000;15:613–20.
60. Eastell R, Christiansen C, Grauer A, et al. Effects of denosumab on bone turnover markers in postmenopausal osteoporosis. Journal of bone and mineral research : the official journal of the American Society for Bone and Mineral Research 2011;26:530–7.
61. Suzuki T, Nakamura Y, Kato H. Effects of denosumab on bone metabolism and bone mineral density with anti-TNF inhibitors, tocilizumab, or abatacept in osteoporosis with rheumatoid arthritis. Therapeutics and clinical risk management 2018;14:453–9. [PubMed: 29535527]
62. Raterman HG, Lems WF. Pharmacological Management of Osteoporosis in Rheumatoid Arthritis Patients: A Review of the Literature and Practical Guide. Drugs & aging 2019;36:1061–72. [PubMed: 31541358]
63. Rossini M, Bagnato G, Frediani B, et al. Relationship of focal erosions, bone mineral density, and parathyroid hormone in rheumatoid arthritis. The Journal of rheumatology 2011;38:997–1002. [PubMed: 21459948]

64. Solomon DH, Kay J, Duryea J, et al. Effects of Teriparatide on Joint Erosions in Rheumatoid Arthritis: A Randomized Controlled Trial. Arthritis & rheumatology 2017;69:1741–50. [PubMed: 28544807]

65. Bouta EM, Kuzin I, de Mesy Bentley K, et al. Brief Report: Treatment of Tumor Necrosis Factor-Transgenic Mice With Anti-Tumor Necrosis Factor Restores Lymphatic Contractions, Repairs Lymphatic Vessels, and May Increase Monocyte/Macrophage Egress. Arthritis & rheumatology 2017;69:1187–93. [PubMed: 28118521]

66. Yao Z, Li Y, Yin X, Dong Y, Xing L, Boyce BF. NF-kappaB RelB negatively regulates osteoblast differentiation and bone formation. Journal of bone and mineral research : the official journal of the American Society for Bone and Mineral Research 2014;29:866–77.

67. Dempster DW, Compston JE, Drezner MK, et al. Standardized nomenclature, symbols, and units for bone histomorphometry: a 2012 update of the report of the ASBMR Histomorphometry Nomenclature Committee. Journal of bone and mineral research : the official journal of the American Society for Bone and Mineral Research 2013;28:2–17.

68. Bouxsein ML, Boyd SK, Christiansen BA, Guldberg RE, Jepsen KJ, Muller R. Guidelines for assessment of bone microstructure in rodents using micro-computed tomography. Journal of bone and mineral research : the official journal of the American Society for Bone and Mineral Research 2010;25:1468–86.

69. Kuo TR, Chen CH. Bone biomarker for the clinical assessment of osteoporosis: recent developments and future perspectives. Biomark Res 2017;5:18. [PubMed: 28529755]

70. Li J, Ayoub A, Xiu Y, et al. TGFbeta-induced degradation of TRAF3 in mesenchymal progenitor cells causes age-related osteoporosis. Nature communications 2019;10:2795.

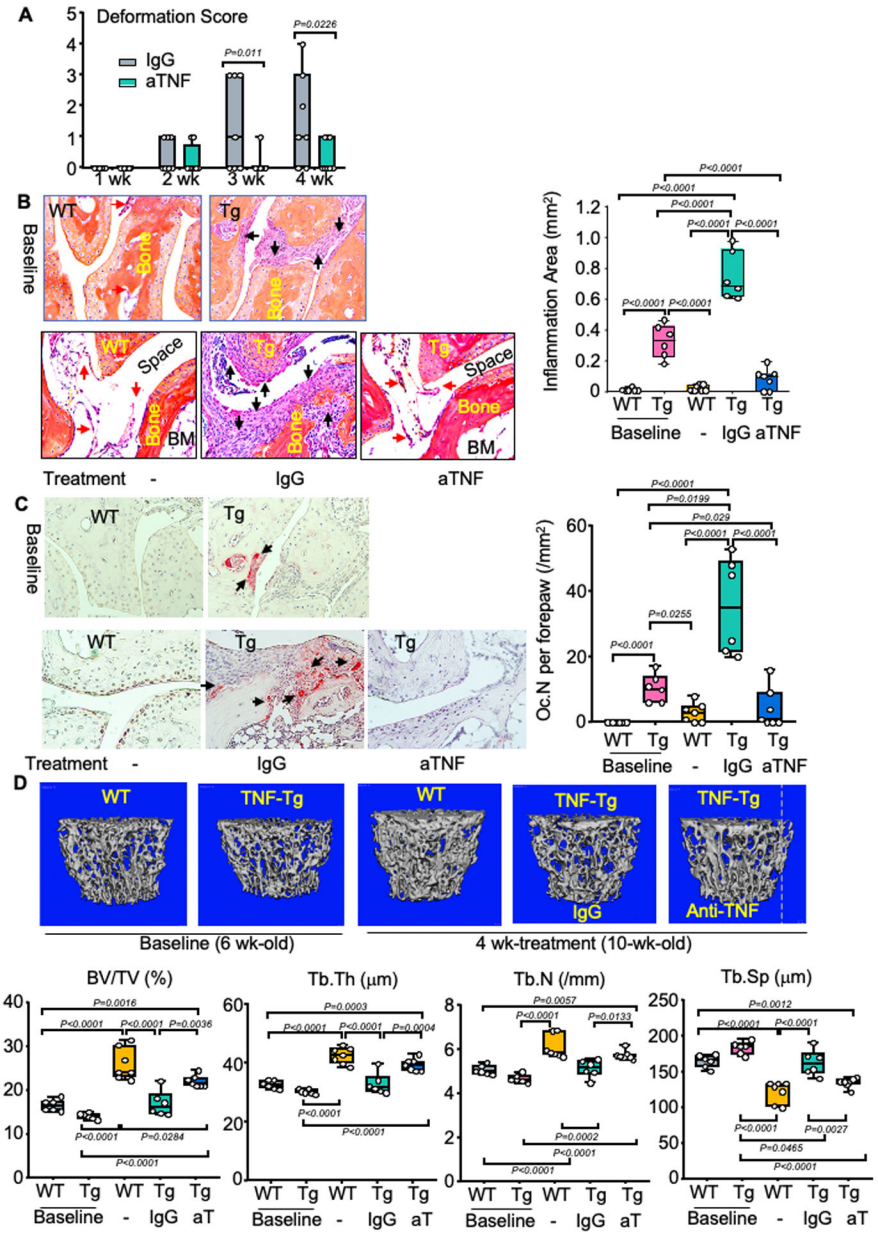

Fig.1. TNF antibody blocks joint erosion, but has limited effect to improve trabecular bone volume in juvenile TNF-Tg mice with initial stage arthritis.

6-wk-old female TNF-Tg mice were treated with normal IgG control or anti-TNF Ab (aTNF), once a wk, for 4 wk. The treated TNF-Tg and WT littermate mice were euthanized on day 29, 7–8 mice per group. 6-wk-old female WT and TNF-Tg mice were used as baseline control. (A) Joint deformation scores in the hind-paws of TNF-Tg mice evaluated blindly once a week. (B) H&E-stained left fore-paw sections used to evaluate inflammatory tissue infiltration into the joints, articular cartilage and carpal bones. Black arrow: normal synovial tissue extending to the joint space; Yellow arrow: inflammatory tissues developed on the connective tissue between bones; Red arrow: inflammatory tissues eroding cartilage and bone. (C) TRAP-stained left fore-paw sections were used to evaluate number of osteoclast (OC) (black arrow) in the inflammatory tissue infiltrating the joints, cartilage and

bone. (D) Representative micro-CT images of L1 vertebrae (upper panel) and quantification of bone structural parameters: bone mass (BV/TV), trabecular number (Tb.N), trabecular thickness (Tb.Th) and trabecular separation (Tb.Sp) (lower panel). Base = baseline. Group size: 6 mice for both WT and Tg at baseline; treatment WT control 6, IgG 6 and aTNF 7 mice. Each dot represents the data from one mouse. p values are shown between two groups.

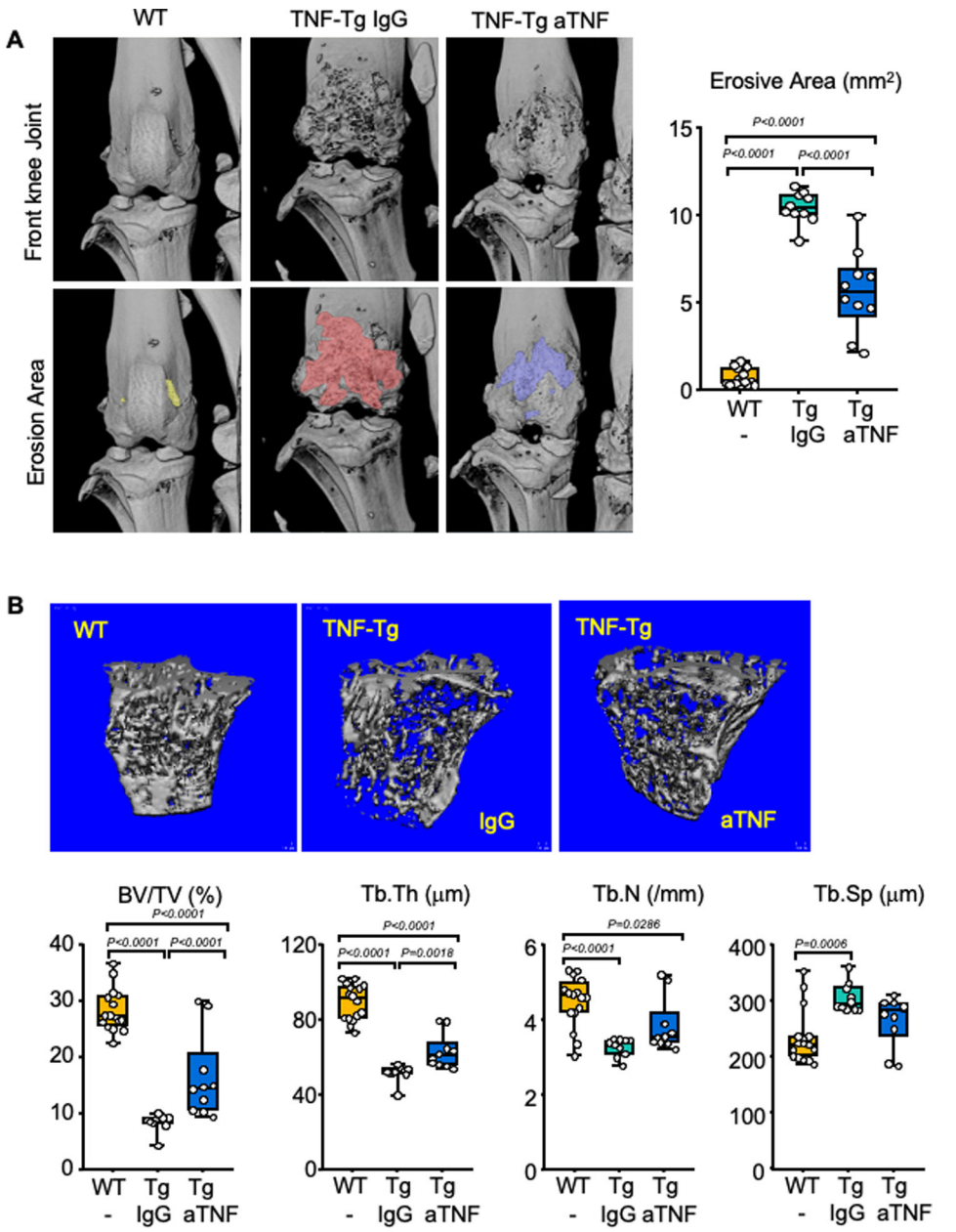

Fig.2. TNF Ab has limited effect to increase trabecular bone mass in adult TNF-Tg mice with advanced erosive arthritis.

8-m-old TNF-Tg mice were treated with normal IgG control or anti-TNF antibody (aTNF), once a wk, for 5 wk. (A) Micro-CT scanned datasets (DICOM) of both knee joints were imported into Amira software to analyze the erosive area on the front of distal femora. (B) Representative micro-CT images and bone structural parameters, BV/TV), Tb.N, Tb.Th and Tb.Sp, in a 200 μm long region starting at 100 μm beneath the growth plate in the proximal tibia. Sample size: 8 WT control mice, 5 TNF-Tg mice for each IgG and aTNF; both legs from all the mice were scanned with micro-CT, and each dot represent the data from one leg.

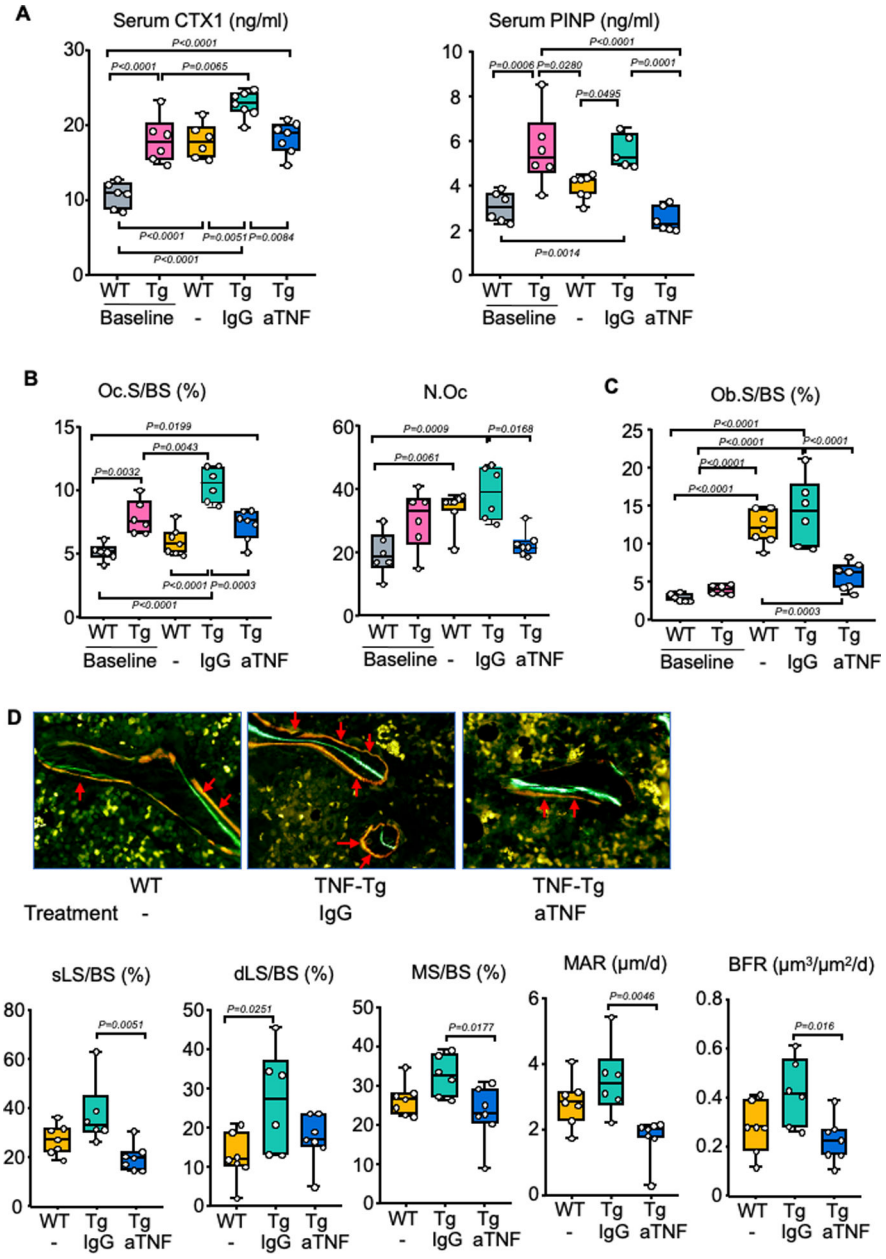

Fig.3. TNF Ab reduces bone turnover in TNF-Tg mice.

(A) Serum samples from the mice, as in Fig.1, used to test the bone resorption marker, CTX1, and bone formation marker, PINP. (B) Osteoclast surfaces (Oc.S) and numbers (Oc.N) were measured on TRAP-stained left tibial sections. (C) Osteoblast surfaces (Ob.S) were measured on H&E-stained left tibial sections. (D) Right tibiae were processed as plastic sections. Upper panel: representative images of calcein-alizaren Red double labeling (Red arrows); lower panel: quantification of dynamic bone formation parameters: single-labeled surface (sLS/BS), double-labeled surface (dLS/BS), mineralizing surface (MS/BS), mineral apposition rate (MAR) and bone formation rate (BFR). Red arrows indicate double labels. Sample number in each group was same to Fig.1.

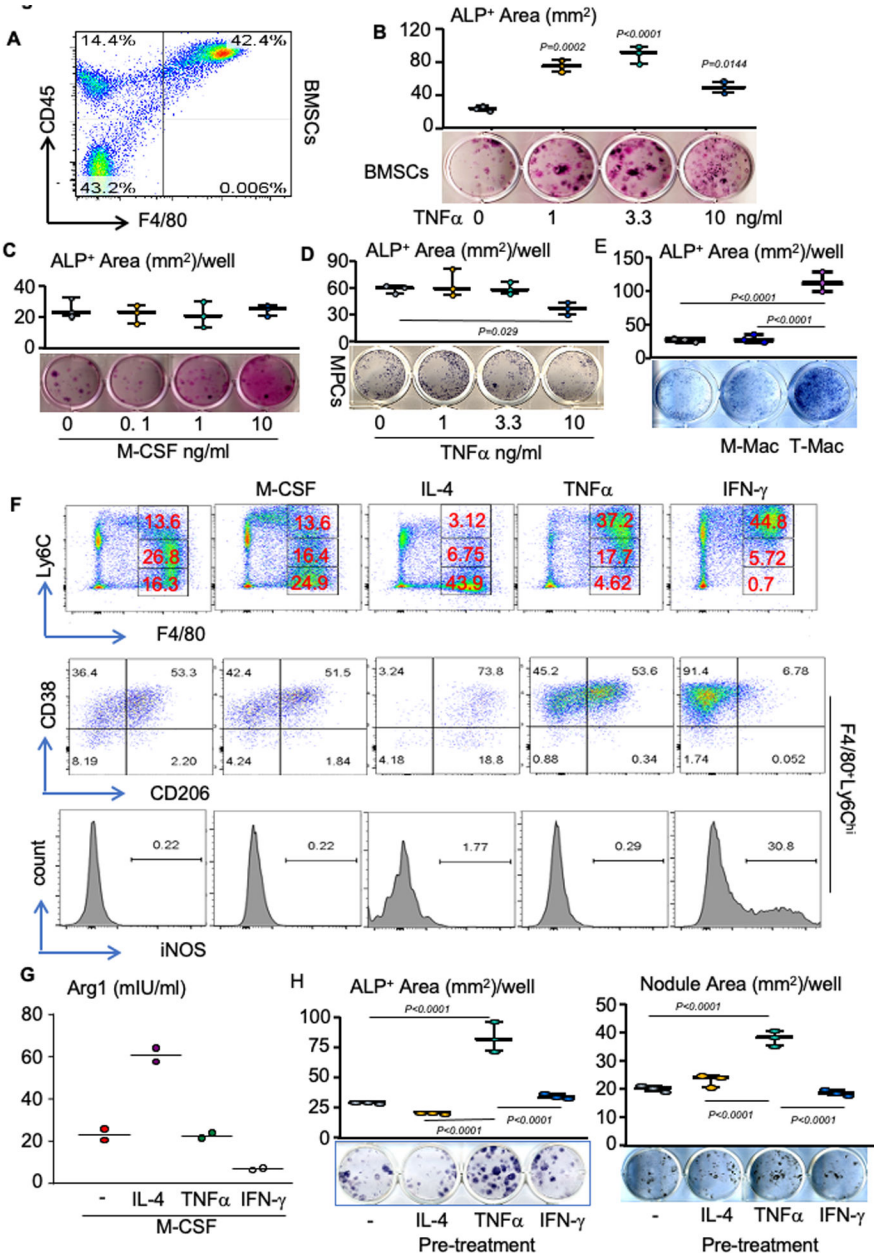

Fig.4. TNF-polarized macrophages stimulate OB differentiation.

(A) 1×10^6 BM cells from C57Bl6 WT mice cultured for 5 d to expand BM stromal cells (BMSCs) and flow cytometry for CD45 and F4/80 expression. (B)&(C) BMSCs were expanded in the presence of TNFα or M-CSF for 5 d, as in (A), followed by OB induction for 5 d without cytokines. ALP followed by eosin staining to quantify ALP^+ OB area, p value vs. un-treated. (D) Pure mesenchymal progenitor cells (pMPCs) cultured from bone of C57Bl6 WT mice induced for OB differentiation to quantify ALP^+ OB area, as in (B), p value vs. un-treated. (E) 5×10^3 PBMCs/well in 24-well plates cultured with 1 ng/ml M-CSF or in combination with 3.3 ng/ml TNFα for 6 d to induce or polarize Macs (M- or T-Macs). Culture medium with cytokines was removed, and 5×10^4 pMPCs were added and induced for OB differentiation, as in (A), from the second day for 7 d. ALP staining to

quantify ALP^+ OB area. (F) BMSCs were expanded, as in (A), in the presence of 3 ng/ml M-CSF, IL-4, TNFα or IFN-γ for 5 d. Markers of macrophage polarization measured by flow cytometry. (G) Arg1 concentration in culture medium of the BM cells expanded by the indicated cytokines, as in (F), tested by ELISA. (H) BMSCs expanded in the presence of indicated cytokines for 5 d, as in (F), followed by induction of OB differentiation for 7 and 12 d to evaluate ALP^+ OB area. (left panel) and mineralized nodule formation (right panel, Von Kossa staining), respectively. All in vitro experiments were repeated 3 times with similar results. Data in (G) was from two independent experiments and the other data were the representative of 3 repeated experiments with similar results.

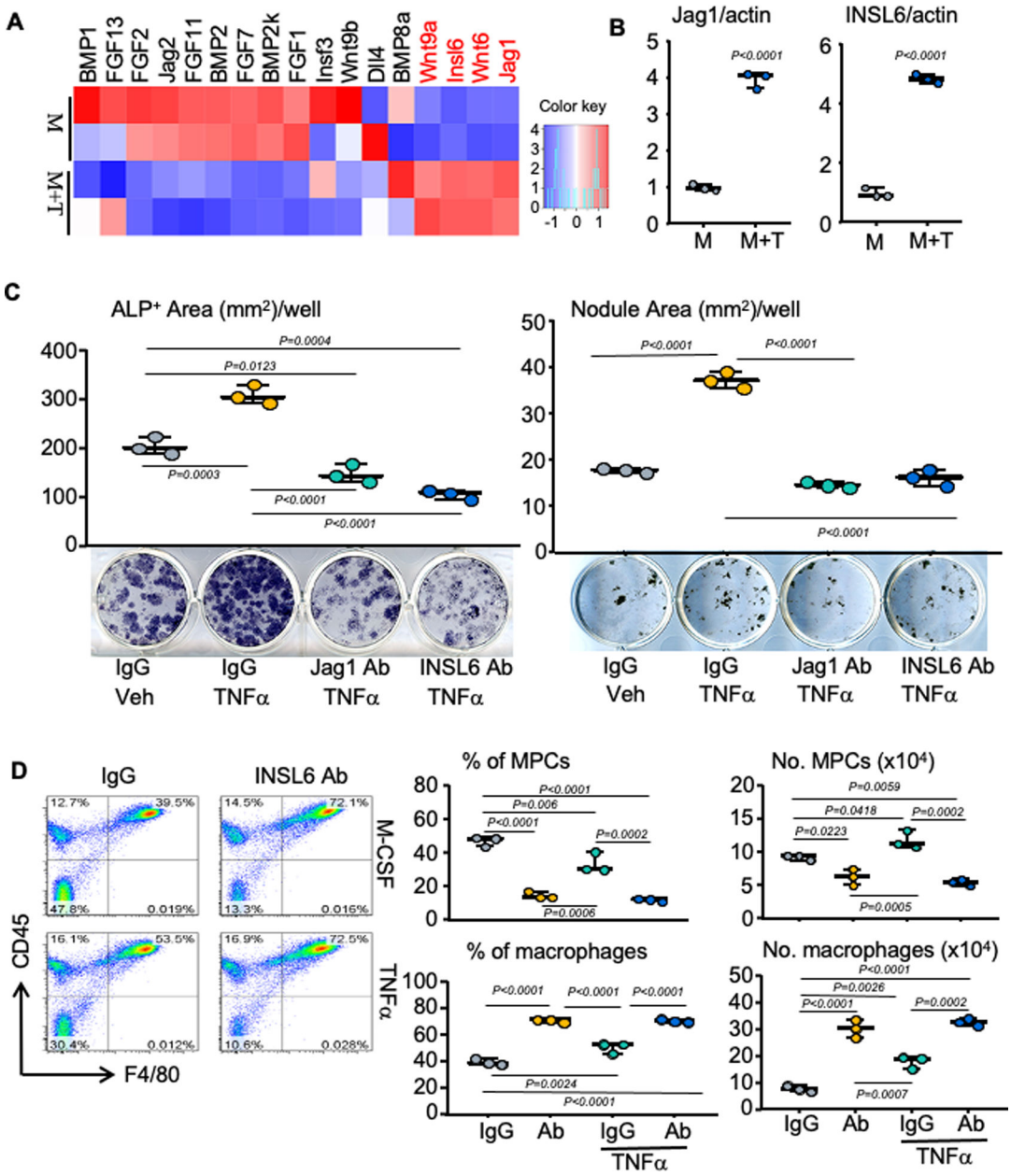

Fig.5. TNF-polarized macrophages produce INSL6 to stimulate OB differentiation by expanding mesenchymal progenitor cells.

(A) Total RNA extracted from cultured mouse macrophages treated with M-CSF or M-CSF+TNFα (M+T). RNA-seq analysis to identify the factors that regulate OB differentiation. (B) Jagged1 and INSL6 mRNA in macrophages, as in (A), tested by real-time PCR. (C) BMSCs expanded for 5 d in 12-well plates pre-coated with IgG, Jagged1 Ab or INSL6 Ab followed by OB differentiation for additional 6 and 12 d to quantify ALP+ OB and mineralized nodule area after ALP and Von Kossa staining, respectively. (D) BMSCs expanded for 5 d in 6-well plates pre-coated with IgG or INSL6 Ab. % and number of $CD45^{-}$ mesenchymal progenitor cells (MPCs) and $CD45^{+}F4/80^{+}$ macrophages analyzed by

flow cytometry. The quantitative data were the representative of 3 repeated experiments with similar results.

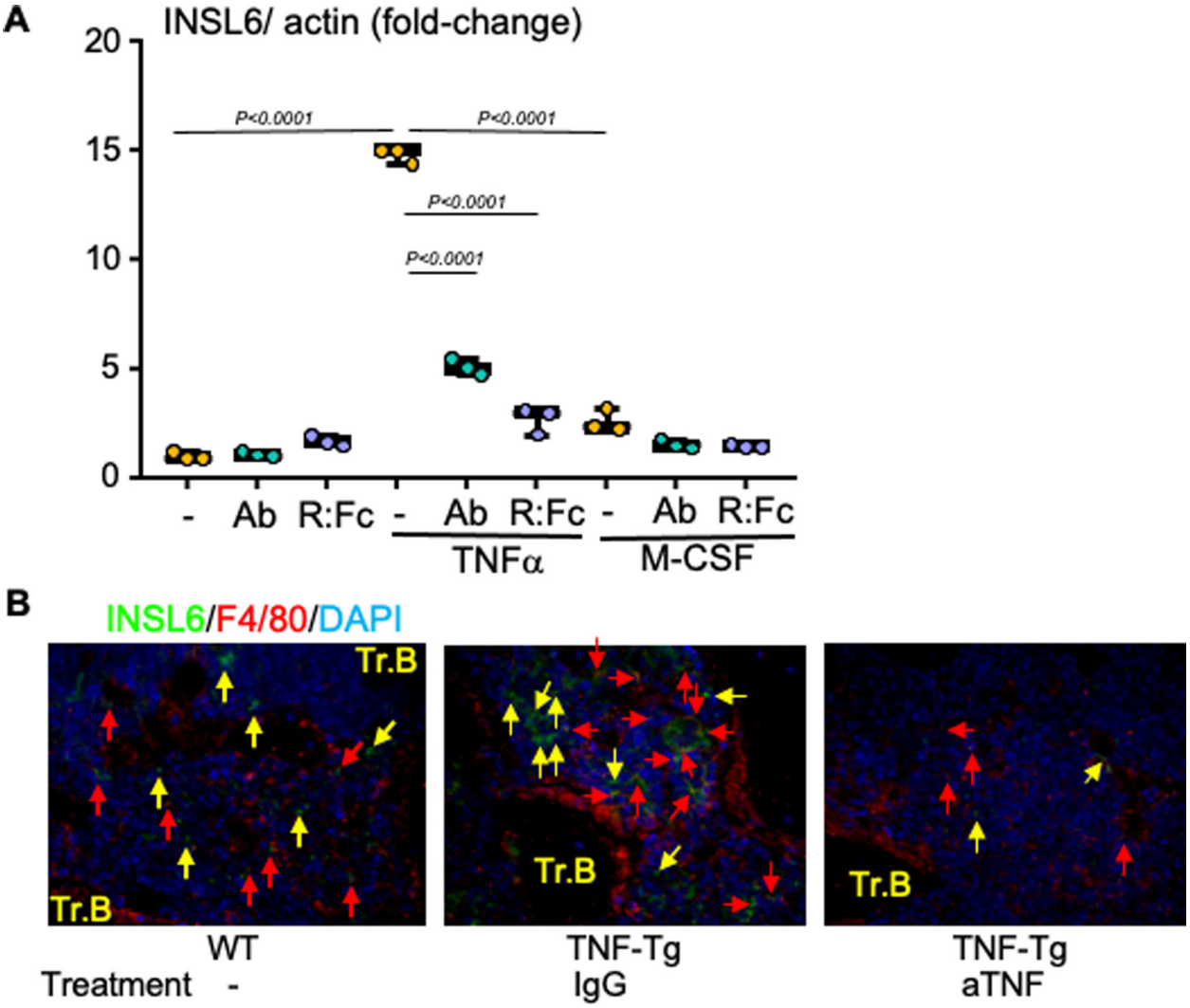

Fig.6. Anti-TNF therapy reduces INSL6 expression by macrophages.

(A) BM cells cultured with TNFα or M-CSF −/+ TNF Ab or TNFR:Fc for 3 d. INSL6 mRNA tested by real-time PCR. (B) Tibial bone sections from WT and TNF-Tg mice treated with IgG or TNF Ab, as in Fig.1, immunostained with Abs against INSL6 and F4/80, with DAPI counterstaining. Red arrows: F4/80^{+} Macs expressing INSL6 (yellow to light red cells); Yellow arrows: non-Mac cells expressing INSL6 (bright green cells). Tr.B = Trabecular bone. R:Fc = TNFR:Fc.